Journal of Biomaterials Science, Polymer Edition

ISSN: (Print) (Online) Journal homepage: https://www.tandfonline.com/loi/tbsp20

Development of hydrogel-forming microneedles for transdermal delivery of albendazole from liquid reservoir

Anugerah Yaumil Ramadhani Aziz, Nurul Afia Hasir, Nurul Bahari Putri Imran, Muhammad Firdaus Hamdan, Ulfah Mahfufah, Nurfadilla Wafiah, Andi Arjuna, Rifka Nurul Utami & Andi Dian Permana

To cite this article: Anugerah Yaumil Ramadhani Aziz, Nurul Afia Hasir, Nurul Bahari Putri Imran, Muhammad Firdaus Hamdan, Ulfah Mahfufah, Nurfadilla Wafiah, Andi Arjuna, Rifka Nurul Utami & Andi Dian Permana (2022): Development of hydrogel-forming microneedles for transdermal delivery of albendazole from liquid reservoir, Journal of Biomaterials Science, Polymer Edition, DOI: 10.1080/09205063.2022.2157671

To link to this article: https://doi.org/10.1080/09205063.2022.2157671

Published online: 18 Dec 2022.

JOURNAL OF BIOMATERIALS SCIENCE, POLYMER EDITION
https://doi.org/10.1080/09205063.2022.2157671

Development of hydrogel-forming microneedles for transdermal delivery of albendazole from liquid reservoir

Anugerah Yaumil Ramadhani Aziz, Nurul Afia Hasir, Nurul Bahari Putri Imran, Muhammad Firdaus Hamdan, Ulfah Mahfufah, Nurfadilla Wafiah, Andi Arjuna, Rifka Nurul Utami and Andi Dian Permana

Faculty of Pharmacy, Hasanuddin University, Makassar, Indonesia

ABSTRACT

Albendazole (ABZ) is an anthelmintic agent from the benzimidazole group, known as the broad-spectrum antiparasitic drug. ABZ is commonly used to treat human intestinal and systemic infections. Orally administered ABZ tends to have limited efficacy due to its poor solubility. In order to enhance its delivery to the therapeutic target, polyvinyl alcohol-based hydrogel-forming microneedles (HFMs) was developed. HFMs can effectively deliver drugs loaded in the reservoir through the transdermal route with fewer side effects and longer therapeutic duration. In addition, to enhance ABZ's solubility, the drug can be loaded as a liquid reservoir using water-miscible solvents, which will effectively enhance the solubility of ABZ, resulting in higher bioavailability. In this study, HFMs was successfully developed with high swelling abilities, more than 400%. Moreover, the penetration result showed HFMs could penetrate up to 63% into the skin with only a 7.14% of height decrease. The skin integrity test also showed HFMs permeation into the skin, causing no changes in skin integrity after 24 h of application. Incorporated with the liquid reservoir, the *ex vivo* permeation test showed that the cumulative amount of ABZ permeated through the skin was about $971.23 \pm 11.77\ \mu g/cm^2$. In conclusion, this innovation has a huge potential to overcome the limitations of ABZ in oral preparations and potentially enhance its therapeutic effect through the transdermal route.

ARTICLE HISTORY
Received 24 September 2022
Accepted 8 December 2022

KEYWORDS
Albendazole; polyvinyl alcohol; hydrogel-forming microneedles; liquid reservoir; transdermal delivery

1. Introduction

Albendazole (ABZ) is a broad-spectrum antiparasitic agent used as the first-line treatment for both intestinal and systemic infections in humans. In the treatment of various systemic infections, ABZ is also known to be widely used as a first-line treatment of echinococcal infections [1]. As anthelmintic agent, ABZ is commonly found in oral preparations [2]. However, according to Biopharmaceutical Classification System (BCS), ABZ had been categorized as borderline BCS class II/IV, having low solubility

CONTACT Andi Dian Permana andi.dian.permana@farmasi.unhas.ac.id Faculty of Pharmacy, Hasanuddin University, Makassar 90245, Indonesia.

and being entirely insoluble in water and most organic solvents [3]. Previous studies [4,5] have shown that ABZ is a weak base whose solubility depends on the solvent's pH. Following oral administration, its solubility will drop sharply in gastric (pH 1.4) and intestinal fluids (pH 6.5), resulting in poor bioavailability and limited drug efficacy. As a result, ABZ is often delivered as high-dose oral preparations, resulting in more adverse effects, especially in patients with poor liver function. Recorded between 2006 and 2015, according to The Korean Institute of Drug Safety & Risk Management data, there were 256 probable or possible adverse effects caused by ABZ in oral preparation [5]. Therefore, oral administration of ABZ has become a significant burden due to its severe adverse effects.

Developing another formulation with an improved drug administration route is essential to enhance the delivery of ABZ into infectious areas in the body. The skin, the human body's largest organ, provides a large area for drug absorption. The transdermal route has long been extensively studied and has been praised foremostly for its ease of application. The transdermal drug delivery is a potential drug administration route that offers some promising benefits, including the ability to rapidly deliver drugs to the target with the avoidance of first-pass metabolism [4]. Thus, within this transdermal route, the drug can be delivered to the desired target, suppressing unwanted side effects [6]. Considering the existence of *stratum corneum* that may limit several drugs' permeation [7], preparing pharmaceutical dosage forms through microneedles (MNs) would be an optimum option [8].

MNs are minimally invasive arrays consisting of numerous micron-sized needles assembled on a baseplate, which can penetrate through the stratum corneum and enable drug penetration [9]. Among other drug administrations, MNs typically only require a low dose to achieve the therapeutic effect [10,11]. Furthermore, such MNs are painless and may be more comfortable for the patient during therapy. In terms of storage stability, MNs is widely known to be able to maintain its stability even without specialized storage condition. Previous study [12] showed that MNs had no significant loss of the drugs during storage at 25 °C for up to 1 year and exposure to 60 °C for 4 months.

Currently, MNs are widely developed and have multiple types with different advantages. One of the MNs types used recently due to their vast benefits is hydrogel-forming microneedles (HFMs). Hydrogel known to has a physical similarity to human tissue, easily to degraded, and has been widely used for deliver drugs [13,14]. HFMs can offer transdermal drug delivery by readily uptake the interstitial fluid in the human body. HFMs also have a higher drug loading capacity than conventional MNs and offer a tunable drug release rate. Either by incorporating drugs into its polymeric structure or loading drugs into a reservoir, HFMs can effectively be used for transdermal drug delivery. More importantly, HFMs can function as a rate-controlling membrane, allowing sustained drug delivery [15]. The first HFM was developed by Donnelly Research Group using from aqueous blends containing poly(-methyl vinyl ether-co-maleic anhydride) and poly(ethylene glycol) [8]. Furthermore, the application of HMF has been widely used to deliver numerous drugs [10, 14–18].

In terms of material, a biodegradable polymer was added as the base of HFMs. Polyvinyl alcohol (PVA) is one of the most used polymers in biomedical

applications systems and devices due to its water solubility, low toxicity, biocompatibility, excellent physical properties, and known to be able to overcome various problems associated with safety and disposal due to its biodegradable characteristic [16–18]. One study explained that PVA would deposit under the skin after MN administration [19]. Additionally, it was found that after six days, the deposition concentration of PVA in the insertion sites gradually decreased and disappeared entirely from the skin after 28 days of application. However, there were never recorded cases associated with the accumulation of PVA in the skin or drained the lymph nodes at the application site [20]. Due to its vast advantages, PVA was chosen as a suitable HFMs-base used in this study.

Incorporating with the HFMs, drugs can be loaded into the reservoir-base and permeate into the skin through the MNs [15]. In this study, ABZ was formulated into a liquid reservoir using water-miscible solvents to enhance its solubility. The liquid reservoirs were formulated in three different formulations using the combination of PEG 400 and PEG 600. The previous study [25] shows that using PEG 400 and co-solvent could rapidly increase the solubility of ABZ. Adding co-solvents will enhance the drug solubility by reducing the polarity of the entire system [4]. Thus, the formulation of ABZ into a liquid reservoir could be considered as an appropriate option. Generally, this study aims to develop a novel transdermal delivery of ABZ with rapid and higher permeation across the stratum corneum using HFMs incorporated with a liquid reservoir.

2. Materials and methods

2.1. Materials

ABZ (purity, ≥98+%) of analytical grade was purchased from Alfa Aesar (Lancashire, UK). PVA (typically average M_w = 72,000 g/mol), sodium alginate (SA) (medium viscosity), and carbomer 980 were purchased from Sigma-Aldrich Pte Ltd. (Singapore, Singapore). Polyvinylpyrrolidone (PVP) K-30 was purchased from Fadjar Kimia (Bogor, Indonesia). Poly(ethylene glycol) (PEG 600 Da), tartaric acid, absolute ethanol, glycerin, and propylene glycol were purchased from Merck Schuchardt OHG (Hohenbrunn, Germany). PEG 400 and Tween80® were purchased from idCHEM Co., Ltd. (Gyeonggi, South Korea). Tablet phosphate-buffered saline (PBS) used in the swelling and dissolution study was purchased from Dulbecco A Oxoid Ltd. (Hampshire, UK). Silicon template, ST-08 10 × 10 array, was purchased from Micropoint Technologies P.T.E. Ltd. All other chemicals and materials used in this study were of analytical grade.

2.2. Fabrication of chemically cross-linked hydrogels

Chemically cross-linked hydrogels were fabricated from an aqueous polymeric blend containing PVA, PVP K30, carbomer 980, and tartaric acid. Different proportions of each compound were showed in Table 1. Based on previous studies [27], the use of PVA and PVP in the hydrogel formulation is known to produce MNs with optimal characteristics. In addition, carbomers can build hydrogen bonds between the

Table 1. Formulation of chemically cross-linked hydrogels.

	Formulation code		
Compositions (%w/w)	H1	H2	H3
PVA	10	15	20
PVP K30	10	10	10
Carbomer 980	1	1	1
Tartaric acid	1.5	1.5	1.5
Deionized water	77.5	72.5	67.5

Table 2. Formulation of physically cross-linked hydrogels.

	Formulation code	
Compositions (%w/w)	H4	H5
Sodium alginate (1.5%)	30	70
PVA (10%)	70	30

carbomer's carboxyl group and the PVA's hydroxyl group, resulting in a stronger hydrogel bond. Carbomer can also increase the viscosity of the formula due to the presence of hydrogen bonds which can produce MNs with better mechanical strength and swelling ability [28]. As a cross-linking agent, tartaric acid containing carboxyl and hydroxyl groups which can build an active site in the non-covalent interaction bond, producing a hydrogel with good cohesive properties [29].

The polymer solution was made by mixing PVA and PVP K30, then heated at 80 °C until a clear solution was obtained. Then, the carbomer (prepared by swelling it overnight on the deionized water) and tartaric acid were added to the solution. Finally, the mixture was poured into the petri dish and dried for two days at 37 °C. After drying, the hydrogels were separated from the petri dish and heated at 120 °C for 2 h [27].

2.3. Fabrication of physically cross-linked hydrogels

Physically cross-linked hydrogels were prepared by a freezing-thaw method according to the procedure explained in the previous study [30]. An aqueous solution containing 1.5% (w/v) SA and 10% (w/v) PVA was dissolved using deionized water. Different proportions of SA and PVA (Table 2) were mixed and vortexed until fully dissolved. A proper amount of the mixture was poured into a petri dish, freezing at −20 °C for 18 h and thawing at 25 °C for 6 h (three continuous cycles).

2.4 Swelling studies of hydrogels

The swelling of hydrogel was investigated using a 1 cm^2 hydrogel film over 24 h at room temperature. The hydrogel was prepared using the methods previously explained in Sections 2.2 and 2.3. Each dry hydrogel was weighed (m_o) and placed in a glass containing 30 mL of PBS (pH 7.4). At intervals 0.5, 1, 2, 3, 4, 5, 10, 15, 30, 45, 60, 120, 180, 240, 300, 360, 420, 480, and 1440 min, each hydrogel was removed from

the excess solution of PBS using tissue paper and then weighed (m_t). The percentage of swelling was calculated by using the following equation:

$$\% \text{ Swelling } = \left(\frac{m_t - m_o}{m_o}\right) \times 100\% \tag{1}$$

2.5. Determination of gel fraction

The obtained hydrogel was dried in an oven at 50 °C for 24 h and weighed as W_0. Then, soaked the hydrogel in distilled water for 24 h and dried again at 50 °C and weighed as W_e [30]. The gel fraction (GF%) was calculated by using the equation below:

$$\text{Gel fraction } (\text{GF}\%) = (W_e/W_o) \times 100 \tag{2}$$

2.6. Water vapor transmission

Water vapor transmission (WVT) studies were carried out using glass vials as the transmission cells. About 1 g of anhydrous fused calcium chloride was initially put into dried glass vials. Then, the hydrogel was taped over the brim of the transmission cells. Furthermore, the vials were weighed and then located to the desiccators containing saturated potassium chloride solution [31]. After the predetermined time, the transmission cells were weighed again, and the WVT was determined using the following equation:

$$\text{WVT} = \frac{\text{Mass of the vial} \times \text{thickness of the hydrogel}}{\text{Surface area of the hydrogel}} \tag{3}$$

2.7. Surface pH

The surface pH test was carried out by weighing 20 mg of hydrogel into a beaker containing 50 mL of distilled water. Then, the hydrogel was let rise at room temperature for 15 min, and the combined electrode near the surface of the HFMs was measured after an equilibration time of 1 min [6].

2.8. Moisture absorption ability

Moisture absorption ability was conducted by using a 1 cm^2 hydrogel. The hydrogels were then placed in three different conditions of relative humidity (RH), i.e. desiccators containing magnesium chloride (33% RH), sodium nitrite (69% RH), and potassium sulfate (97% RH). Every 24 h within 14 days, each hydrogel was weighed, and the percentage of moisture absorption ability was calculated by using the equation below:

$$\%\text{MAA} = \frac{\text{The final mass of hydrogel} - \text{the initial mass of hydrogel}}{\text{The initial mass of hydrogel}} \tag{4}$$

2.9. Fabrication of HFMs

HFMs were fabricated using the same method explained in Sections 2.2 and 2.3, except for using a petri dish as the mold. Each 0.5 g of every formula, as shown in Tables 1 and 2, was poured onto the mold (Silicone template ST-08 10 × 10 array, 700 µm height) and degassed using a centrifuge at 3500 rpm for 10–20 min. For the chemical cross-linking process, each silicone mold containing the formula (Table 1) was dried for two days at 37 °C. After drying, the HFMs were separated from the silicone mold and heated at 120 °C for 2 h. Meanwhile, for the physical cross-linking process, every mold containing formula (Table 2) was frozen at −20 °C for 18 h and thawed at 25 °C for 6 h, repeatedly for three continuous cycles.

2.10. Characterization of HFMs

The penetration test was carried out using eight layers of Parafilm® (≈1 mm; 126 μm/layer). HFMs were attached and lowered onto the eight sheets of Parafilm® and given a load until it met the required force of 32 N, exerted and held for 30 s. Following the penetration test, the Parafilm® sheets were unfolded. Then, the number of holes formed in each layer of Parafilm® was counted [32,33].

A mechanical strength test was carried out using a similar method to the penetration test. The HFMs was placed on eight layers of Parafilm® and given a load of 32 N for 30 s. The MN height before and after the mechanical strength test was compared by using the optical microscope (Olympus® CX23 LED) and changes were determined using Image J software (National Instrument of Health, USA) [34].

2.11. Fourier transform infrared (FTIR) spectroscopy analysis

FTIR spectroscopy was used to investigate the compatibility of ABZ with all types of excipients used in this study. All the samples were analyzed using FTIR Accutrac FT/IR-4100 Series (Jasco, Essex, UK) [6].

2.12. Saturation solubility

The saturation solubility of ABZ was carried out using the shake-flask method [4]. An excess drug was added to the solvent in glass vials. Then, all vials were vortex-mixed for 10 min and ABZ was added to the vial continuously until the solvent was saturated. The vial was then placed in a rotary incubator at 37 °C for 24 h at 40 rpm. After 24 h, each sample was analyzed using ultraviolet–visible (UV–vis) spectrophotometry. Solvents chosen and tested in this study included several organic solvents, i.e. PEG 400, PEG 600, ethanol, glycerol, and propylene glycol. This test was also carried out using water to compare the solubility of ABZ in water and other organic solvents.

2.13. Swelling studies of HFMs in organic solvents

The swelling of HFMs in potential organic solvents was conducted using the same method previously explained in Section 2.4. HFMs was weighed (m_o), then placed in

Table 3. Formulation of ABZ liquid reservoirs.

	Formulation code		
Compositions (%w/w)	F1	F2	F3
ABZ	1	1	1
PEG 400	99	–	49.5
PEG 600	–	99	49.5

a glass containing 30 mL of chosen organic solvents. At regular intervals, each HFM was removed from excess solvents using tissue paper and then weighed (m_t). The swelling percentage was calculated by using Equation (1).

2.14. Formulation of the liquid reservoir

The liquid reservoirs were prepared according to the formulation shown in Table 3. In various concentrations, PEG 400 and PEG 600 were poured into the glass vial. Then, ABZ was added to the mixture and vortex-mixing vigorously until homogenous.

2.15. Ex vivo permeation study

All the animals used in this study were treated based on the protocol approved by the Research Ethics Committee, Faculty of Medicine, Hasanuddin University, Indonesia. One day before the *ex vivo* permeation study, the rats were euthanized. The abdominal skin was cut out, and the fat layer was removed from the skin, obtaining skins with the thickness of 1.32 ± 0.1 mm. Then, the skin was washed using PBS solution (pH 7.4) repeatedly, and the skin thickness was measured using a digital caliper (Taffware® LCD-XY, Indonesia), obtaining skins with the thickness of 1.32 ± 0.1 mm. Afterward, the skin was wrapped in aluminum foil and placed in the freezer (−20 °C) for further testing.

Ex vivo permeation test was carried out using 2% of Tween80® dispersed in PBS (pH 7.4) at 37 °C to ensure sink conditions [34]. Using Tween80® as a surfactant will improve the solubility of ABZ during the dissolution studies. In addition, a dissolution medium containing surfactant can better simulate *in vivo* conditions compared to other non-physiological agents or organic solvents [35]. Unfortunately, the conventional Franz cell setup is unsuitable for investigating the permeation ability of liquid reservoirs incorporated with HFMs. A traditional Franz cell setup limits the liquid reservoir's movement to permeate into the skin through the MNs. Then, the various modifications of the Franz cell setup were done using the method described in the previous study [4]. The schematic representation of the modified Franz cell setup was shown in Figure 1. In order to calculate the amount of drug release, the samples were then analyzed using UV–vis spectrophotometry at the maximum wavelength. The cumulative drug release was then fitted into different mathematical kinetic models, as seen in the equations below [36]:

$$\begin{aligned} &\text{Zero-order kinetics} && Q_t = Q_0 + K_0 t \\ &\text{First-order kinetics} && \ln Q_t = \ln Q_0 - K_1 t \\ &\text{Higuchi model} && Q_t = K_H \times t^{1/2} \\ &\text{Korsmeyer-Peppas model} && Q_t = K t^n \\ &\text{Hixson-Crowell model} && {Q_0}^{1/3} = {Q_0}^{1/3} - {Q_t}^{1/3} = K_s t \end{aligned} \tag{5}$$

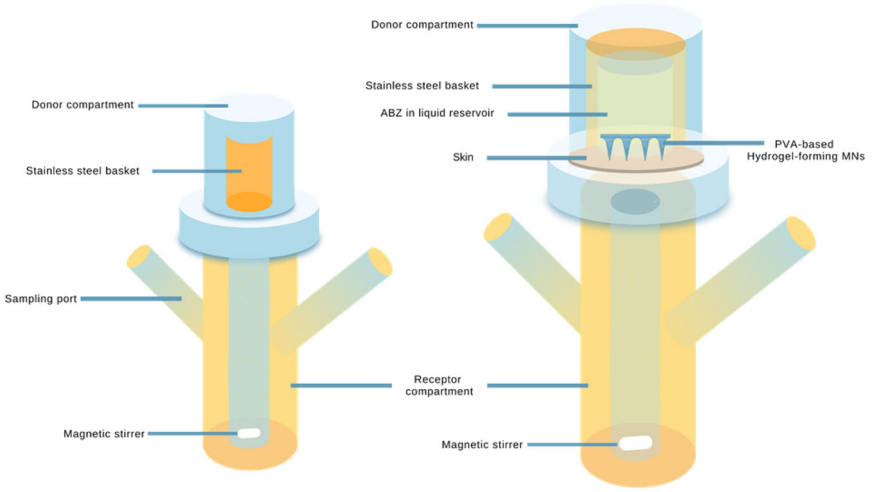

Figure 1. Schematic representation of modified Franz cell setup for *ex vivo* permeation study using stainless steel basket cylinder.

Q_t (%) showed the percentage of drug released at the time (t), Q_0 is the starting value of Q_t and n is the diffusion release exponent. The value of flux (J) and coefficient of permeation (K_p) can be calculated using Equation (6) [37]. All data of permeation results were calculated using DDsolver.

$$J = Q/A \times t$$
$$K_p = Q/[A \times (C_0 - C_i)] \quad (6)$$

2.16. Skin integrity test

A skin integrity test was conducted to investigate the effect of HFMs application after 24 h of *ex vivo* permeation study [38]. The skin's integrity was evaluated using FTIR spectroscopy at a wavelength of 400 to 4000 cm^1 using FTIR Accutrac FT/IR-4100 Series (Jasco, Essex, UK). At the end of *the ex vivo* permeation study, the skin was washed and analyzed using FTIR spectroscopy. Furthermore, the untreated skin was used as a negative control.

2.17. Statistical analysis

All methods were calculated using Microsoft® Excel® 2019 (Microsoft Corporation, Redmond, USA) to determine the mean and SD. Statistical analysis was performed using IBM® SPSS® Statistics 26.0 (IBM, Armonk, New York, USA). Based on statistical analysis, $p \leq 0.05$ was considered statistically significant in all cases. Premium GraphPad Prism® version 9.2 (GraphPad Software, CA, USA) was used to create graphs from obtained data.

3. Results and discussions

3.1. Fabrication of hydrogel and in vitro swelling studies

HFMs offer a promising better administration of drugs with the minimally invasive approach that adequately enhances the drug's therapeutic effect due to its capability

to form a hydrogel network between each polymeric material [27]. In this study, PVA is essential since it is a water-soluble polymer and slightly soluble in ethanol, implying that it has a high potential as a good hydrogel base material. This polymer constitutes a hydrophilic structure, making it capable of taking up a large amount of water in its three-dimensional polymeric network. Combined with other polymers, such as PVP K30 and carbomer, the formed hydrogel will potentially provide better swell behavior when inserted into the skin due to the presence of interstitial fluid [39]. Generally, the swelling study is one vital parameter to determine the characteristic of the HFMs. The swelling properties of the hydrogel are defined by several factors, such as the polymer concentration, cross-linker type, or cross-linking ratio. In this case, the concentration of PVA used was variated (Tables 1 and 2) to determine its effect on hydrogel's swelling properties [40]

The swelling profile of hydrogel in PBS (pH 7.4) was presented in Figure 2(A). PBS was chosen as the standard swelling medium to represent the interstitial fluid of the human body [30]. The combined formula of PVA and SA (H4 and H5) was dissolved immediately after contact with the PBS solution (data not shown). The ideal formula of HFMs should maintain its integrity and have good swelling properties in PBS (pH 7.4) [9]. Thus, the physically cross-linked hydrogel formulations were omitted from further studies. Otherwise, the formula containing PVA, PVP, carbomer, water, and tartaric acid (H1, H2, and H3) showed pleasant swelling in PBS. The covalent bonds of those polymers caused the HFMs to not dissolve in the interstitial fluid yet showed high swelling behavior [30].

Figure 2(A) compares the swelling percentage (%) of H1, H2, and H3. Based on the results, it is evident that the swelling rate of H1 was superior when compared to the other formulations. Statistical analysis showed that the swelling percentage of H1 was significantly higher than H3 ($p < 0.05$). This observation is supported by previous research that explained about the PVA concentration, which was known to substantially affect the swelling behavior of hydrogel. Higher PVA concentration means more sites are available for cross-linking [41]. This can be seen in the lower swelling rate of H2 and H3, shown in Figure 2(A), due to the lower PVA concentration than H1. An increase in PVA concentration will lead to the rise of medium viscosity, thereby limiting PVA chain movement. Hence, this will hinder the ability of the polymer matrix to absorb water [42].

3.2. Gel fraction of hydrogel

Generally, the gel fraction (GF) describes the flexibility of the hydrogel. Hydrogel with low flexibility may indicate complex characteristics and difficulty in absorbing liquid, including interstitial fluid [30]. GF also calculates the degree of grafting in each hydrogel formula [43]. Based on the GF determination test, it was found that the GF (%) of H1 ($95.45 \pm 0.26\%$), H2 ($87.70 \pm 0.35\%$), and H3 ($85 \pm 0.07\%$) were in the acceptable range. H1 and H3 differed significantly in GF percentage ($p < 0.05$). The obtained result showed that the GF% monotonically decreased with the increase in PVA concentration.

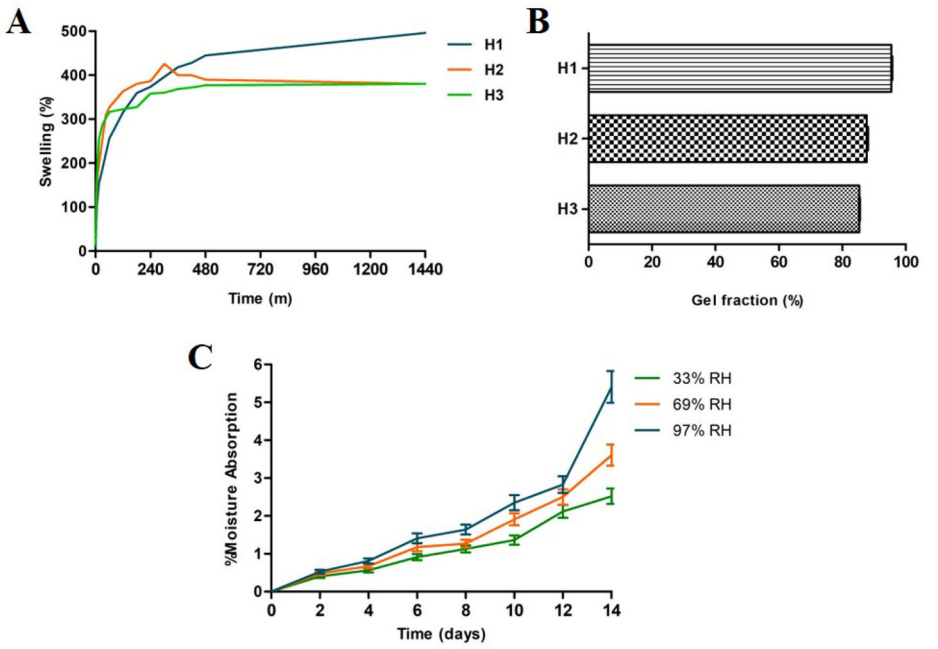

Figure 2. (A) Swelling percentage of HFMs in PBS (pH 7.4); (B) gel fraction percentage of HFMs (means ± SD); (C) moisture absorption of H1 at 33% RH, 69% RH, and 97% RH (means ± SD).

Furthermore, the GF% provides more information about the cross-linking process' effectiveness in forming an insoluble fraction. As shown in Table 1, H1 only consist of 10% of PVA (%w/w) and H3 of PVA (%w/w) up to 20%. The increase in GF percentage implies that this parameter primarily depends on the concentration of PVA, which leads to better cross-linking properties and a higher ability to form an insoluble fraction [44]. A further increase in PVA concentration of about 5% (%w/w) could decrease the swelling capacity due to the viscosity increase, limiting the PVA chain and reducing the water absorption capacity [42].

3.3. Water vapor transmission

WVT test was conducted to determine the hydrogel's permeability characteristics, showing the quantity of moisture transmitted through the unit area of the hydrogel in unit time. After seven days, the WVT rate turned out to be 0.53 ± 0.04 mg cm/cm^2 at 24 h, indicating that the H1 formulation was permeable to water vapor, probably due to the PVP content which is one of the hygroscopic polymers. However, this WVT rate is still considered low and potentially indicates the hydrogel's long-term stability [31, 45].

3.4. Surface pH

Investigating the surface pH of HFMs is very important to ensure that the surface pH of HFMs, which is directly attached to the skin, could not possibly irritate during application [39]. Inappropriate pH values of preparations can potentially irritate the

skin, especially when applied to the skin for an extended time. Thus, it is essential to conduct the surface pH test of HFMs. The result showed that the surface pH value of H1 is about 5.32 ± 0.49, close to the skin's pH around 5.8 [46]. This implied that the HFMs could be applied to the skin without causing any irritation.

3.5. Moisture absorption ability

Moisture absorption indicated hydrogel's affinity to uptake the external water molecules. In addition, the higher moisture absorption rate may affect the functionality of MNs under storage conditions. Based on the results shown in Figure 2(C), the higher RH values directly affect the increase of moisture absorption ability of H1. After 14 days of testing, all formulas had a moisture absorption percentage of <10%. It is probably due to the existence of PVP in a hydrogel formulation. PVP is a unique polymer with a strong moisture absorption ability due to its hygroscopic characteristic. In this case, the PVP used in the formulation will directly affect the moisture absorption ability of the hydrogel [47]. Furthermore, the changes in RH can also affect the ability of the hydrogel to absorb the external water. Generally, the higher RH in the environment will cause a higher value of moisture absorption [48]. However, the moisture absorption of H1 was still considered low compared to other MNs formulas containing PVP that gained up to 14–16% of moisture absorption [45].

3.6. Characterization of HFMs

Representative H1 of microscopic images are shown in Figures 3 and 5. The penetration and mechanical test have been carried out to determine the strengths and hardness characteristics of HFMs in correlation with their penetration ability to the skin. The formula of H1 was cast onto the mold, dried at 37 °C for 2 days, and then heated at 120 °C for 2 h for cross-linking step. The penetration test showed that each HFMs H1 replicated could penetrate up to the fourth layer of Parafilm® (504 µm) with an average percent penetration reaching up to 63% of the MN height (Figure 3(C)). Along with that percentage, it indicates that HFMs H1 can penetrate through the stratum corneum, passes through the epidermis into the dermis, as the epidermis has a thickness of up to 180 µm [49]. In the case of 32 N applied force, the penetration of the needles into the skin was at its greatest, which showed more than 50% penetration up to the fourth layer of Parafilm®. This result indicates that HFMs H1 was probably hard enough to penetrate and transverse intact to the *stratum corneum*. The obtained result of the mechanical strength test showed a percentage decrease in the height of HFMs H1. After the mechanical strength test, the size of HFMs H1 decreased by only 7.14% of its total height (Figure 3(D)).

3.7. Physicochemical characterization of ABZ and HFMs using FTIR spectroscopy

As shown in Figure 3(E), ABZ was characterized using FTIR spectroscopy. The spectra showed the N-H stretching in 3350–3310 cm^{-1} and the peak at 3332.99 cm^{-1}. It was also noticed that the valence vibrations of the aromatic were found in the range

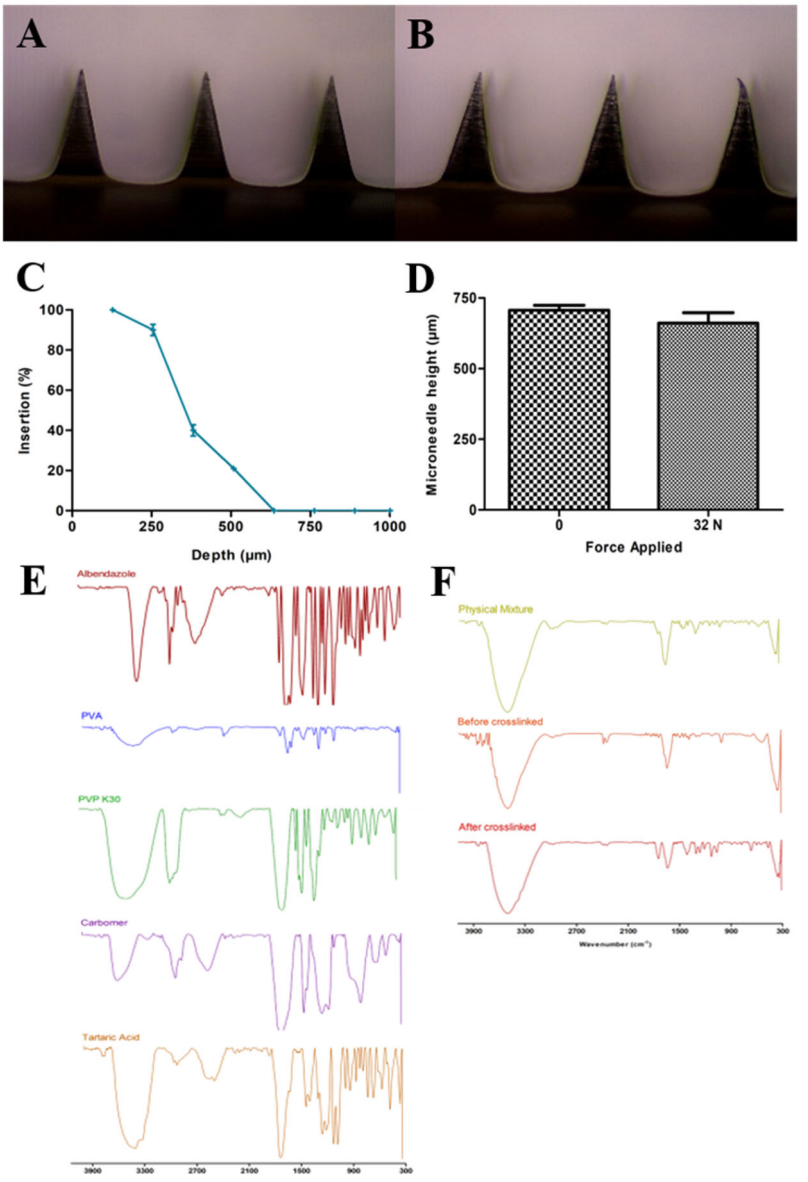

Figure 3. Microscopic observation of HFMs H1 (4× magnification) (A) before mechanical strength test; (B) after mechanical strength test; (C) penetration test results of HFMs H1 (means + SD, $n = 3$); (D) comparison of HFMs H1 height before and after mechanical strength test (means ± SD, $n = 3$); FTIR spectra of (E) ABZ's spectra and each composition of H1; (F) physical mixture of HFMs H1, before and after-crosslinked process of H1.

of 1650–2000 cm^{-1}. Around 1500–1700 cm^{-1}, the valence vibration of the group carboxyl C = O from the ester group appeared. Moreover, the valence vibrations of the C–O stretching were identified in the 1250–1310 cm^{-1} from group ester, and the peak showed at 1192.01 cm^{-1}.

In the fabrication of hydrogel for drug administration, the cross-linking process can directly affect the properties of each component of HFMs. To determine the

cross-linking effects on the structure of each polymer, infrared (IR) spectroscopy was used in this study. The spectra of HFMs containing polymer and cross-linker agent were presented in Figure 3(E). As for the comparison between pre- and post-cross-linked HFMs, the spectra were shown in Figure 3(F). The critical difference between IR spectra of pre- and post-crosslinked HFMs can be found in the presence of new band between 1750 and 1500 cm^{-1}. This range was known as the carbonyl region. The pre-crosslinked HFMs presented only a single peak in the carbonyl region. Thus, the spectra of post-crosslinked HFMs showed two different carbonyl peaks. The new peak was shown at ca. 1730 cm^{-1}, which can be identified as new ester cross-link bonds. This unique bond can be formed due to the esterification process between the reaction of hydroxyl groups of PVA and carboxylic groups of tartaric acid during the cross-linking process [50].

As shown in Figure 3(F), the intermolecular interactions of tartaric acid molecules with PVA polymer chains are shown by several inter- and intramolecular cross-links formed. The position of the band shifted, and the absorbance of this band increased significantly with the increase of tartaric acid content, indicating an increase in cross-link density in the structure. The absorbance of the carbonyl group increased with increasing TA concentration due to the esterification process. The cross-linking of the PVA chains reduces the hydroxyl groups of the PVA chains and forms new cross-linked ester bonds with the carbonyl strain [50].

3.8. Saturation solubility

The solubility of ABZ in some potential organic solvents was carried out to determine the most suitable reservoir medium to use incorporated with HFMs H1. The saturation solubility of ABZ was conducted to provide a more detailed understanding of the solubility of ABZ. The solubility was tested in several organic solvents that could potentially enhance the absorption and bioavailability of ABZ in the liquid reservoir.

As shown in Figure 4(A), the results showed that the highest ABZ solubility was found in a mixture of ABZ with ethanol, PEG 400, and PEG 600. The results of ABZ solubility in ethanol compared to PEG 400 and PEG 600 were significantly different ($p < 0.05$). The ABZ solubility in ethanol was shown to be the highest. In contrast, the solubility of ABZ at PEG 400 and PEG 600 was not statistically significant ($p > 0.05$). Therefore, to determine the most appropriate solvent for the liquid reservoir of ABZ, those three different solvents were used for the swelling test using HFMs H1.

3.9. Swelling studies of HFMs in organic solvent and preparation of liquid reservoir

Drugs with poor solubility in water face major issues during pharmaceutical fabrication. Those drugs commonly need to be dissolved into the gastrointestinal fluids to enhance oral bioavailability. The poorly soluble drug often results in limited solubility in gastrointestinal fluid and lower oral bioavailability and absorption [51]. Many strategies have been developed to improve the bioavailability of poorly soluble drugs,

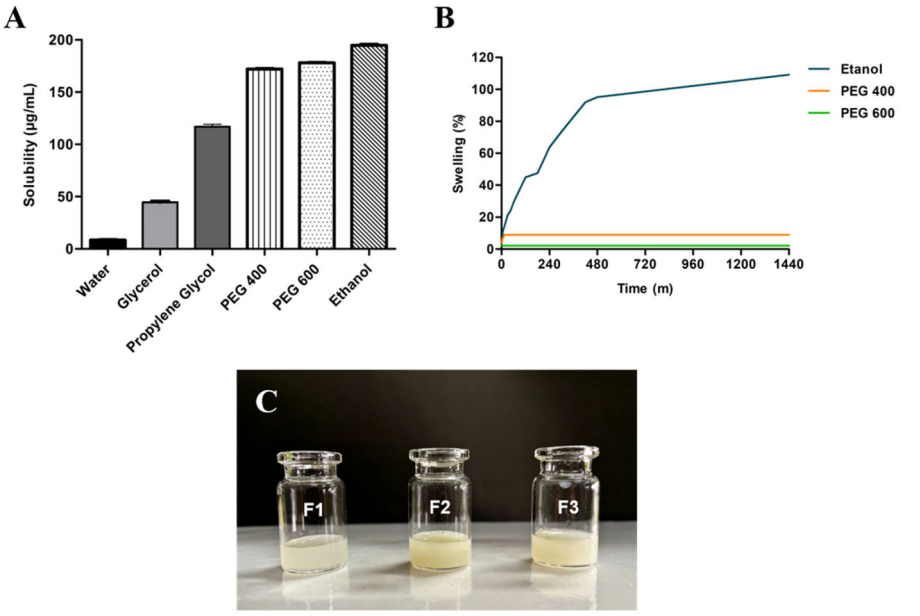

Figure 4. (A) Solubility of ABZ in several organic solvents; (B) swelling percentage of HFMs H1 in potential organic solvents; (C) physical appearance of the liquid reservoir.

including loading the drug in a liquid reservoir by using a non-polar solvent. In the liquid reservoir, adding a non-polar solvent will reduce the system's polarity, enhancing the solubility of the poorly soluble drug [4].

In order to fabricate the liquid reservoir, a swelling test of HFMs H1 in 100% organic solvent was carried out in PEG 400, PEG 600, and ethanol to identify the suitable reservoir medium for the liquid reservoir. The results showed that the highest percentage of swelling rate was found in ethanol compared to PEG 400 and PEG 600, and the obtained results were statistically significant ($p < 0.05$). A suitable reservoir medium in a liquid reservoir incorporated with HFMs must unfound the swelling of HFMs, to ensure that HFMs can only swell upon contact with the body's interstitial fluid [4]. Therefore, based on the results of the swelling test in 100% organic solvents, as shown in Figure 4(B), PEG 400 and PEG 600 were chosen as the most suitable reservoir medium.

3.10. Ex vivo permeation study

The *ex vivo* permeation test was conducted to determine the permeation profile of each formula of liquid reservoir integrated with HFMs H1. The accumulative permeation of ABZ at 24 h from each formula was F1 (865.43 ± 5.95 µg/cm^2), F2 (869.06 ± 25.46 µg/cm^2), and F3 (971.23 ± 11.77 µg/cm^2) (Figure 5(A)).

The value of the permeation coefficient (P) in Table 4 also describes the amount of ABZ permeated per unit of concentration described in cm/h. As evident from the results in Figure 5(A), F3 provided a better drug flux across the skin than F1 and F2. Therefore, considering the cumulative amount of ABZ permeated through the skin

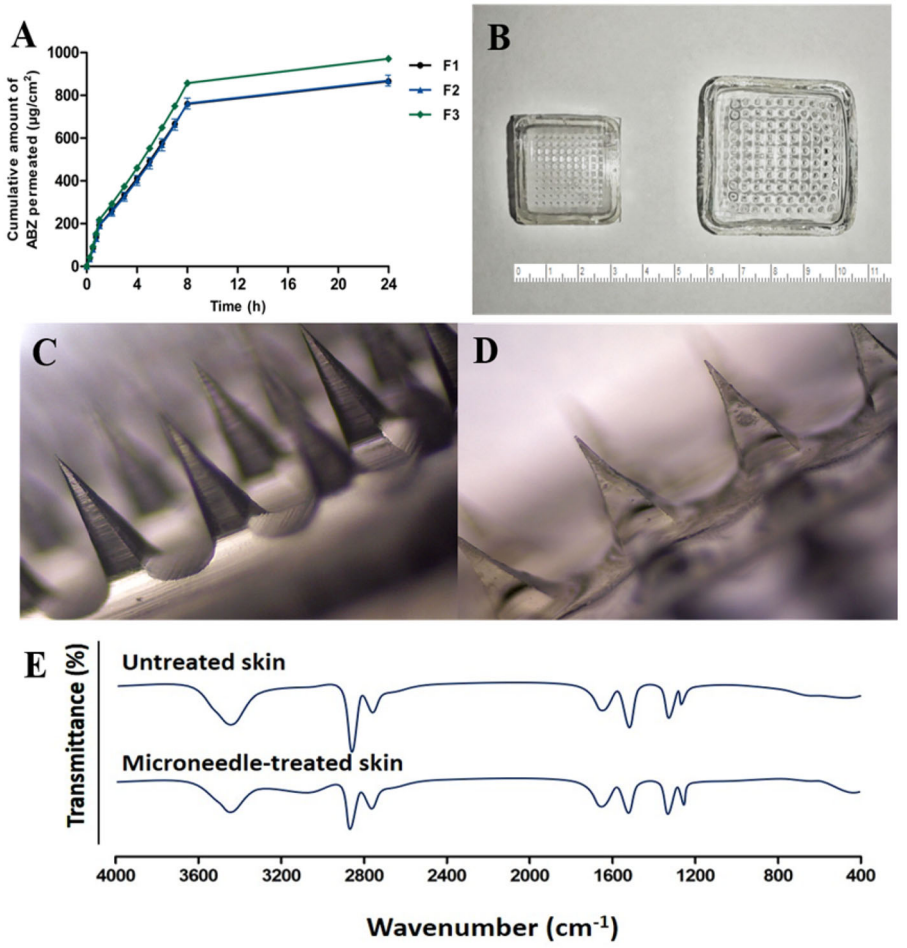

Figure 5. (A) *Ex vivo* permeation profiles of HFMs H1 incorporated with the liquid reservoir F3; (B) macroscopic comparison of HFMs pre- and post-swelling; Microscopic view of HFMs H1 (4× magnification); (C) before *ex vivo* permeation test; (D) after *ex vivo* permeation test; (E) FTIR spectra of integrity evaluation (comparing the untreated and microneedle-treated skin).

Table 4. Permeation parameter of ABZ liquid reservoir in infinite dose condition.

	Parameter	
Formula	*P* (cm/h) ± SD	*J* (μg/cm²/h) ± SD
F1	285.39 ± 4.13	4.40 ± 0.06
F2	290.26 ± 0.00	4.47 ± 0.00
F3	303.57 ± 13.32	4.68 ± 0.21

membrane, the combination of HFMs H1 and reservoir F3 was consider as the most appropriate combination for delivering ABZ through the transdermal route by using HFMs and liquid reservoir in this study.

To determine the mechanism of ABZ release from HFMs incorporated with a liquid reservoir, the permeation data were analyzed using several different kinetic models (zero order, first order, Higuchi, Hixson–Crowell, and Korsmeyer–Peppas).

The results showed the release of ABZ following the Korsmeyer–Peppas kinetic model with a correlation coefficient value (R^2) is 0.95. In the Korsmeyer–Peppas kinetic model, the value of n determines the mechanism of drug release. The value of n found in this permeation test is 0.217. The value of $n < 0.5$ indicates the mechanism of drug release by Fickian diffusion [52–54]. In that sense, the release of ABZ depended on the diffusion of liquid that occurs through the swollen matrix of HFMs, which could be generated by the relaxation of polymer chains [55].

3.11. Skin integrity test

The integrity evaluation result using FTIR is shown in Figure 5(E). Comparing the untreated and MN-treated skin, a significant difference was found in the presence of new peaks at 2915 and 2760 cm^{-1} in the untreated skin. These ranges were also known as hydrocarbon areas, which were present due to the asymmetric hydrocarbon stretching and symmetric CH_2 stretching. This hydrocarbon area represents the ceramide and the fatty acid in the stratum corneum. Furthermore, the amide I and amide II bonds were also discovered in the corneocytes' keratin at 1679 and 1513 cm^{-1}. According to Figure 5(E), all those peaks were also present in MN-treated skin with insignificant changes in all intensities. Based on the obtained result above, it was concluded that the administration of HFMs did not change the integrity of the skin after 24 h of application and is considered safe to be used in drug administration.

In development of HFMs as potential drug administration, considering the translation of this technology is one of the critical points. After many years of studies and researches, there are many significant developments of MNs technology commercialization [21]. Currently, there are some devices containing MNs by both the academic and industrial researchers alike which are waiting for FDA approval [51]. Therefore, another thing that needs to be considered is the sterilization issue of the HFMs. Previous study has shown that repeated application of MNs into the skin did not cause any decrease on the skin barrier function. The administration of MNs also did not cause the microorganism to penetrate through the skin. Moreover, it has been reported that the use of polymer-based MNs, such as HFMNs, would not stimulate the humoral immune system and considered to be safe even after repeated applications. It could be concluded that the risk of infection was consider low in the administration of HFMs. However, more research needs to be conducted to ensure the effectiveness, therapeutic safety, and the sterilization issues of HFMs [52].

Unlike common conventional transdermal drug delivery systems, the combination of HFMs and liquid reservoir have high potential to reduce the risk of cross-contamination, which is often appearing during repeated application of other conventional drug administration [26,53]. After being inserted through the skin, the HFMs will absorb the interstitial fluid and swell, then the ABZ loaded in the reservoir will permeate into the cell through passive diffusion [13]. Then, the HFMs will directly be removed from the skin and the ABZ will be delivered to the systemic circulation. Most of ABZ will be excreted through bile and a small portion will be excreted through urine. With that being said, the use of the HFMs and its reservoir are not

designed to be use reproducibly, resulting in low possibility of cross-contamination. In addition, this innovation also tends to increase the convenience of patient due to its ease of application. Considering the acceptance and patient convenience, the HFMs are preferred to be inserted by hand. Previous study [28] shows that insertion of MNs by hand tend to be easier and resulting in better patient compliance. However, in order to penetrate through the stratum corneum, the MNs need to be pressed with certain force, so the use of a pressure-indicating sensor can be an alternative option. Based on previous study, the minimum pressure required for the application of 1 cm^2 of MNs to be able to penetrate to the stratum corneum is 32 N/cm^2. The pressure-indicating sensor will change its color when the applied forces reach 30 N and even be more concentrated if given a greater force [22] [52].

Moreover, the most challenging problem on HFMs fabrication was also the availability of low-cost manufacturing methods [54]. In this study, we used various materials, such as PVA, with several beneficial advantages and considered to be more affordable than other polymers to reduce the cost manufacturing [24]. Regarding about the manufacturing and distribution challenges of MNs, many clinical trials and advancement of MNs technologies proved that MNs could be potentially use for commercial. In addition, there are some of MNs devices which already reached the commercial market for both diagnostic and therapeutic applications [23,55].

4. Conclusion

HFMs incorporated with a liquid reservoir containing ABZ have been successfully formulated using the combination of PVA, PVP K30, carbomer, and tartaric acid as chemical cross-linker. The obtained result of HFMs has been evaluated based on the mechanical properties, swelling profile, gel fraction, water vapor transmission, surface pH, moisture absorption ability, FTIR studies, *ex vivo* permeation study, and skin integrity test. The overall result of this study showed the promising advantages of using HFMs incorporated with a liquid reservoir to overcome the limitations of ABZ in oral administration. Furthermore, *in vivo* pharmacokinetic, pharmacodynamic, and toxicity tests should be conducted in appropriate animal models to investigate this innovation's effectiveness and safety for future commercial use.

Disclosure statement

No potential conflict of interest was reported by the author(s).

Funding

This study was fully funded by Lembaga Penelitian dan Pengabdian kepada Masyarakat (LPPM), Hasanuddin University, Indonesia, through 'Penelitian Dosen Penasehat Akademik (PDPA)' program.

ORCID

Andi Dian Permana http://orcid.org/0000-0002-0063-077X

References

[1] Permana AD, Paredes AJ, Zanutto FV, et al. Albendazole nanocrystal-based dissolving microneedles with improved pharmacokinetic performance for enhanced treatment of cystic echinococcosis. ACS Appl Mater Interfaces. 2021;13(32):38745–38760.

[2] Hong ST. Albendazole and praziquantel: review and safety monitoring in Korea. Infect Chemother. 2018;50(1):1–10.

[3] Pettarin M, Bolger MB, Chronowska M, et al. A combined in vitro in-silico approach to predict the oral bioavailability of borderline BCS class II/IV weak base albendazole and its main metabolite albendazole sulfoxide. Eur J Pharm Sci. 2020;155:105552.

[4] Kearney MC, McKenna PE, Quinn HL, et al. Design and development of liquid drug reservoirs for microneedle delivery of poorly soluble drug molecules. Pharmaceutics. 2019;11(11):605.

[5] Hu C, Zhang F, Fan H. Improvement of the bioavailability and anti-hepatic alveolar echinococcosis effect of albendazole-isethionate/hypromellose acetate succinate (HPMC-AS) complex. Antimicrob Agents Chemother. 2021;65(7):e02233.

[6] Ananda PWR, Elim D, Zaman HS, et al. Combination of transdermal patches and solid microneedles for improved transdermal delivery of primaquine. Int J Pharm. 2021;609: 121204.

[7] Ning X, Wiraja C, Chew WTS, et al. Transdermal delivery of chinese herbal medicine extract using dissolvable microneedles for hypertrophic scar treatment. Acta Pharm Sin B. 2021;11(9):2937–2944.

[8] Coulman S, Allender C, Birchall J. Microneedles and other physical methods for overcoming the stratum corneum barrier for cutaneous gene therapy. Crit Rev Ther Drug Carr Syst. 2006;23(3):205–258.

[9] Donnelly RF, Singh TRR, Garland MJ, et al. Hydrogel-forming microneedle arrays for enhanced transdermal drug delivery. Adv Funct Mater. 2012;22(23):4879–4890.

[10] Anjani QK, Sabri AB, Utomo E, et al. Elucidating the impact of surfactants on the performance of dissolving microneedle array patches. Mol Pharm. 2022;19(4):1191–1208.

[11] Donnelly RF, McCrudden MTC, Alkilani AZ, et al. Hydrogel-forming microneedles prepared from 'super swelling' polymers combined with lyophilised wafers for transdermal drug delivery. PLoS One. 2014;9(10):e111547.

[12] Mistilis MJ, Joyce JC, Esser ES, et al. Long-term stability of influenza vaccine in a dissolving microneedle patch. Drug Deliv Transl Res. 2017;7(2):195–205.

[13] Li Z, Chen Z, Chen H, et al. Polyphenol-based hydrogels: pyramid evolution from crosslinked structures to biomedical applications and the reverse design. Bioact Mater. 2022;17:49–70.

[14] Wei S, Li J, He H, et al. A three-layered hydrogel patch with hierarchy releasing of PLGA nanoparticle drugs decrease neointimal hyperplasia. Smart Mater Med. 2022;3: 139–147.

[15] Turner JG, White LR, Estrela P, et al. Hydrogel-forming microneedles: current advancements and future trends. Macromol Biosci. 2022;21(2):2000307.

[16] Oh NG, Hwang SY, Na YH. Fabrication of a PVA-based hydrogel microneedle patch. ACS Omega. 2022;7(29):25179–25185.

[17] Tekko IA, Chen G, Domínguez-Robles J, et al. Development and characterisation of novel poly (vinyl alcohol)/poly (vinyl pyrrolidone)-based hydrogel-forming microneedle arrays for enhanced and sustained transdermal delivery of methotrexate. Int J Pharm. 2020;586:119580.

[18] Cheung K, Das DB. Microneedles for drug delivery: trends and progress. Drug Deliv. 2016;23(7):2338–2354.

[19] Zhang XP, Wang BB, Li WX, et al. In vivo safety assessment, biodistribution and toxicology of polyvinyl alcohol microneedles with 160-day uninterruptedly applications in mice. Eur J Pharm Biopharm. 2021;160:1–8.

[20] Rouphael NG, Paine M, Mosley R, et al. The safety, immunogenicity, and acceptability of inactivated influenza vaccine delivered by microneedle patch (TIV-MNP 2015): a randomised, partly blinded, placebo-controlled, phase 1 trial. Lancet. 2017;390(10095): 649–658.
[21] Indermun S, Luttge R, Choonara YE, et al. Current advances in the fabrication of microneedles for transdermal delivery. J Control Release. 2014;185:130–138.
[22] Vicente-Pérez EM, Quinn HL, McAlister E, et al. The use of a pressure-indicating sensor film to provide feedback upon hydrogel-forming microneedle array self-application in vivo. Pharm Res. 2016;33(12):3072–3080.
[23] Rad ZF, Prewett PD, Davies GJ. An overview of microneedle applications, materials, and fabrication methods. Beilstein J Nanotechnol. 2021;12:1034–1046.
[24] Tucak A, Sirbubalo M, Hindija L, et al. Microneedles: characteristics, materials, production methods and commercial development. Micromachines. 2020;11(11):961–930.
[25] Meena AK, Sharma K, Kandaswamy M, et al. Formulation development of an albendazole self-emulsifying drug delivery system (SEDDS) with enhanced systemic exposure. Acta Pharm. 2012;62(4):563–580.
[26] Donnelly RF, Raj TR, Singh AZ, et al. Hydrogel-forming microneedle arrays exhibit antimicrobial properties: potential for enhanced patient safety. Int J Pharm. 2013; 451(1–2):76–91.
[27] Pan X, Li Y, Pang W, et al. Preparation, characterisation and comparison of glabridin-loaded hydrogel-forming microneedles by chemical and physical cross-linking. Int J Pharm. 2022;617:121612.
[28] Ahmed Saeed Al-Japairai K, Mahmood S, Hamed Almurisi S, et al. Current trends in polymer microneedle for transdermal drug delivery. Int J Pharm. 2020;587:119673.
[29] Wang D, Yang F, Cong L, et al. Lignin-inspired hydrogel matrixes with adhesion and toughness for all-hydrogel supercapacitors; 2022. Available from SSRN: https://ssrn.com/abstract = 4096790.
[30] Kamoun EA, Kenawy ERS, Tamer TM, et al. Poly (vinyl alcohol)-alginate physically crosslinked hydrogel membranes for wound dressing applications: characterization and bio-evaluation. Arab J Chem. 2015;8(1):38–47.
[31] Singh A, Bali A. Formulation and characterization of transdermal patches for controlled delivery of duloxetine hydrochloride. J Anal Sci Technol. 2016;7(1):1–13.
[32] Ripolin A, Quinn J, Larrañeta E, et al. Successful application of large microneedle patches by human volunteers. Int J Pharm. 2017;521(1–2):92–101.
[33] Vora LK, Donnelly RF, Larrañeta E, et al. Novel bilayer dissolving microneedle arrays with concentrated PLGA nano-microparticles for targeted intradermal delivery: proof of concept. J Control Release. 2017;265:93–101.
[34] Abdelghany S, Tekko IA, Vora L, et al. Nanosuspension-based dissolving microneedle arrays for intradermal delivery of curcumin. Pharmaceutics. 2019;11(7):308.
[35] Nagra U, Barkat K, Ashraf MU, et al. Feasibility of enhancing skin permeability of acyclovir through sterile topical lyophilized wafer on self-dissolving microneedle-treated skin. Dose Response. 2022;20(2):15593258221097594.
[36] Paulo C, Lobo JMS. Modeling and comparison of dissolution profiles. Eur J Pharm Sci. 2001;13(2):123–133.
[37] PermeGear Inc. Diffusion testing fundamentals. PermeGear Inc. [Internet]; 2014:1–8. Available from: permegear.com/wp-content/uploads/2015/08/primer.pdf.
[38] Nguyen HX, Bozorg BD, Kim Y, et al. Poly (vinyl alcohol) microneedles: fabrication, characterization, and application for transdermal drug delivery of doxorubicin. Eur J Pharm Biopharm. 2018;129:88–103.
[39] Waghule T, Singhvi G, Dubey SK, et al. Microneedles: a smart approach and increasing potential for transdermal drug delivery system. Biomed Pharmacother. 2019;109: 1249–1258.

[40] Anjani QK, Permana AD, Cárcamo-Martínez Á, et al. Versatility of hydrogel-forming microneedles in in vitro transdermal delivery of tuberculosis drugs. Eur J Pharm Biopharm. 2021;158:294–312.
[41] Yan S, Wang W, Li X, et al. Preparation of mussel-inspired injectable hydrogels based on dual-functionalized alginate with improved adhesive, self-healing, and mechanical properties. J Mater Chem B. 2018;6(40):6377–6390.
[42] Mehrotra T, Zaman MN, Prasad BB, et al. Rapid immobilization of viable Bacillus pseudomycoides in polyvinyl alcohol/glutaraldehyde hydrogel for biological treatment of municipal wastewater. Environ Sci Pollut Res Int. 2020;27(9):9167–9180.
[43] Chen XY, Low HR, Loi XY, et al. Fabrication and evaluation of bacterial nanocellulose/poly(acrylic acid)/graphene oxide composite hydrogel: characterizations and biocompatibility studies for wound dressing. J Biomed Mater Res B Appl Biomater. 2019;107(6):2140–2151.
[44] Bialik-Was K, Pluta K, Malina D, et al. The effect of glycerin content in sodium alginate/poly(vinyl alcohol)-based hydrogels for wound dressing application. Int J Mol Sci. 2021;22(21):12022.
[45] Kathuria H, Lim D, Cai J, et al. Microneedles with tunable dissolution rate. ACS Biomater Sci Eng. 2020;6(9):5061–5068.
[46] Fithri AN, Wijaya DP, Taher T, et al. Optimization of chitosan–tapioca starch composite as polymer in the formulation of gingival mucoadhesive patch film for delivery of gambier (*Uncaria gambir* Roxb) leaf extract. Int J Biol Macromol. 2020;144:289–295.
[47] Rashid FL, Hashim A. Structural, swelling and water absorption properties of new polymer blends for modern applications. Nanosis, Nanomater Nanotehnol. 2021;19:905–912.
[48] Leplingard F, Borne S, Martinelli C, et al. FWM-assisted Raman laser for second-order Raman pumping. Opt. InfoBase Conf. Pap. 2003. p. 431–432.
[49] Sandby-Moller J, Poulsen T, Wulf HC. Epidermal thickness at different body sites: relationship to age, gender, pigmentation, blood content, skin type and smoking habits. Acta Derm Venereol. 2003;83(6):410–413.
[50] Bozdoğan A, Aksakal B, Denktaş C, et al. Prestretching effect and recovery process of polyvinyl alcohol film crosslinked with tartaric acid. J Appl Polym Sci. 2020;137(46):49421–49415.
[51] Vithani K, Jannin V, Pouton CW, et al. Colloidal aspects of dispersion and digestion of self-dispersing lipid-based formulations for poorly water-soluble drugs. Adv Drug Deliv Rev. 2019;142:16–34.
[52] Permanadewi I, Kumoro AC, Wardhani DH, et al. Modelling of controlled drug release in gastrointestinal tract simulation. J Phys Conf Ser. 2019;1295:012063.
[53] Wu IY, Bala S, Škalko-Basnet N, et al. Interpreting non-linear drug diffusion data: utilizing Korsmeyer-Peppas model to study drug release from liposomes. Eur J Pharm Sci. 2019;138:105026.
[54] Li Y, Wang C, Luan Y, et al. Preparation of pH-responsive cellulose nanofibril/sodium alginate based hydrogels for drug release. J Appl Polym Sci. 2022;139(7):51647–51649.
[55] Concha L, Pires ALR, Moraes AM, et al. Cost function analysis applied to different kinetic release models of *Arrabidaea chica* Verlot extract from chitosan/alginate membranes. Polymers. 2022;14(6):1109.